

THE DEVELOPMENT OF A PIEZOELECTRIC DEFECT DETECTION DEVICE THROUGH MATHEMATICAL MODELING APPLIED TO POLYMER COMPOSITE MATERIALS

Mehman Hasanov^{1*}, Natiq Akhmedov², Rasim Bashirov¹, Sahib Piriev¹, Olga Boprav³, Nicat Ismailov¹

¹Azerbaijan Technical University, Baku, Azerbaijan

²Azerbaijan State Economic University (UNEC), Baku, Azerbaijan

³Belarusian State University of Informatics and Radioelectronics, Minsk, Belarus

Abstract. In this research article, the focus is on examining the strength characteristics of polymer composite materials under various stress states. The investigation into the material dissolution process is conducted in two distinct stages. Initially, the article employs a criterion approach to derive explicit formulas for the latent decay time (incubation period) of materials, considering singular, exponential and Abelian kernels of the damage operator. In the subsequent stage, the classical strength condition is applied to establish a Volterra type integral equation, which characterizes the damage process for hereditary materials. These resulting differential equations are then solved with appropriate initial conditions. The study utilizes the obtained results to create time-dependent graphs of the damage parameter and performs comparisons. A piezoelectric defect detection device for polymer composite materials has been proposed through the application of mathematical modeling.

Keywords: *Polymer composite material, dispersion, strength, damage function, damage parameter, structural elements, piezoelectric device.*

Corresponding Author: Mehman Hasanov, Department of Radiotechnics and Telecommunication, Azerbaijan Technical University, Baku, Azerbaijan, Tel.: +994702112283, e-mail: mehman.hasanov@aztu.edu.az

Received: 7 November 2023; **Accepted:** 12 February 2024; **Published:** 15 April 2024.

1. Introduction

Polymer composite materials with diverse compositions are extensively employed in solving a wide range of practical problems, particularly in applications involving unique conditions such as high-temperature environments. These applications encompass various structures like high-temperature pipes, components within gas turbines, nuclear power plant elements and aviation components, among others (Bashirov & Ismailov, 2022; Piriev, 2023; Akhmedov & Yusubova, 2022; Hasanov *et al.*, 2023; Akhmedov, 2021). Regrettably, many of these structures often lack proper consideration of their strength conditions in their design reports, which can lead to unexpected and premature failures during operation (Akhmedov & Yusubova, 2022; Hasanov *et al.*, 2023; Akhmedov, 2021; Boprav *et al.*, 2023; Fionov *et al.*, 2023; Vavilov, 2020). Hence, the operation of structures under unique conditions and utilizing novel polymer composite

How to cite (APA):

Hasanov, M., Akhmedov, N., Bashirov, R., Piriev, S., Boprav, O. & Ismailov, N. (2024). The development of a piezoelectric defect detection device through mathematical modeling applied to polymer composite materials. *New Materials, Compounds and Applications*, 8(1), 62-74 <https://doi.org/10.62476/nmca8162>

materials underscore the significance of assessing their long-term strength. Durability in this context pertains to the gradual degradation of materials over time and addressing degradation stands as one of the most urgent contemporary challenges. The longevity and resilience of these devices are directly contingent on the nature of the degradation process occurring within the device's material. Consequently, a thorough investigation into the dissolution process is an imperative necessity in this field (Akhmedov, 2021; Boiprav *et al.*, 2023; Fionov *et al.*, 2023; Vavilov, 2020; Vavilov, 2022; Chulkov, 2023).

The dispersion process is significantly influenced by the material's structure, making it potentially complex and unstable. Furthermore, the dissolution process is greatly impacted by external factors, including loading conditions, thermal variations, surface effects and more. These external factors, in turn, affect the material's stress state, which is a primary determinant of material dispersion (Hasanov *et al.*, 2023; Akhmedov, 2021; Boiprav *et al.*, 2023; Fionov *et al.*, 2023; Vavilov, 2020; 2022). In the context of material defects, one type of deterioration is associated with random defects that accumulate over time, leading to cumulative damage. This form of deterioration is termed “scattered scattering” (Akhmedov & Yusubova, 2022; Hasanov *et al.*, 2023; Akhmedov, 2021; Boiprav *et al.*, 2023; Fionov *et al.*, 2023). When stress is uniformly distributed, such as in tensile materials, damage increases consistently with volume. However, in non-uniform stress fields, the dissolution process is divided into two stages: latent dissolution (incubation period) and apparent dissolution. Microcracks and other defects emerge during the latent dissolution stage (within a specific time interval $0 \leq t < t^*$), with local disintegration occurring when $t = t^*$. Subsequently, microcracks and other defects scattered around these local disintegration regions coalesce to form macrocracks. For example, experiments on fatigue failure of materials reveal that during the initial stages of failure, damage accumulates gradually and is dispersed. Towards the end of this stage, macrocracks form and propagate rapidly in subsequent moments. In fatigue cracking, the incubation period accounts for 80-90% of the total number of cycles for smooth specimens. The apparent damage stage witnesses relatively rapid disintegration (Piriev, 2023; Akhmedov, 2021).

Two approaches are employed to explore time-dependent dispersion issues in materials. The first approach is the criterion approach, which involves the establishment of criteria to determine the long-term degradation process of materials. These criteria are often based on the concept of “equivalent stress”. The criterion approach is typically used in the analysis of time-independent stress tensor components (Chertishchev, 2020; Slavin *et al.*, 2022). Studies using this approach have been reviewed. However, it has been found that the laws of “deformable solid mechanics” are inadequate for expressing the long-term deterioration of materials under “creep” conditions. Therefore, a second approach, known as the “kinetic method”, has been introduced to address long-term durability concerns (Chertishchev, 2020; Slavin *et al.*, 2022). This approach is founded on the concept of a scalar “damage parameter” function denoted as $\omega(t)$. This function characterizes the material's condition at any given operational time t . The value $\omega(0) = 0$ signifies the material's initial state (prior to use), while $\omega(t^*) = 1$ corresponds to the state of complete material dissolution.

To incorporate the damage function $\omega(t)$ for the uniaxial stress state, let's consider a cylindrical composite material rod with a cross-sectional radius r that is subjected to a stretching force F . We will use the relative change in the cross-section of the cylindrical rod as the damage parameter. The normal stress in the cross-section at time $t=0$ can be expressed as follows,

$$\sigma_0 = \frac{F}{A_0}, \quad (1)$$

the term $A_0 = \pi r^2$ represents the cross-sectional area of the rod at the initial (undamaged) state. As a consequence of the growth of linear dimensions of defects in the cross-section of the bar after loading, the cross-sectional area will start to decrease.

$$A(t) = A_0 - \Delta A(t). \quad (2)$$

In this context, $\Delta A(t)$ is a function that represents the reduction in cross-sectional area as a function of time. Consequently, the normal stress in the cross-section will also vary with time, as it depends on the changing cross-sectional area due to the degradation of the material,

$$\tilde{\sigma}(t) = \frac{F}{A(t)}. \quad (3)$$

By considering (2) in (3)

$$\tilde{\sigma}(t) = \frac{F}{A_0 - \Delta A(t)} = \frac{F}{A_0 \left(1 - \frac{\Delta A(t)}{A_0}\right)}. \quad (4)$$

In here,

$$\omega(t) = \frac{\Delta A(t)}{A_0}. \quad (5)$$

This function is a scalar function that characterizes the damage process. By substituting equation (6) into equation (5), the law governing the variation of normal stress over time can be expressed as follows

$$\tilde{\sigma}(t) = \frac{F}{A_0(1-\omega(t))}. \quad (6)$$

By considering (1) in (7)

$$\tilde{\sigma}(t) = \frac{\sigma_0}{1-\omega(t)}. \quad (7)$$

The utilization of this approach has led to the development of numerous theories regarding the long-term degradation of materials, supported by experiments conducted by various researchers (Bashirov & Ismailov, 2022; Fionov *et al.*, 2023; Chertishchev, 2020; Slavin *et al.*, 2022). However, alongside their advantages, these theories also exhibit limitations, which have been examined in (Akhmedov & Yusubova, 2022; Fionov *et al.*, 2023; Vavilov, 2020; 2022; Chulkov, 2023; Chertishchev, 2020; Slavin *et al.*, 2022; Aamir *et al.*, 2019; Ge *et al.*, 2018; Shukla, 2019).

Theoretical investigations rely on empirical experiments for validation. Diverse experiments were conducted on various materials subjected to different conditions (Bashirov & Ismailov, 2022; Piriev, 2023; Akhmedov & Yusubova, 2022). As an illustration, the dissolution process within tubular metal samples under high-temperature conditions was studied. These works specifically addressed the challenge of the prolonged collapse of composite pipes experiencing both tension and internal pressure.

2. Development of a mathematical model for polymer composite material damage

2.1. A scalar parameter of damage

In the context of developing a mathematical model for the long-term degradation of polymer composite materials under homogeneous stress, a cylindrical rod subjected to a force F and with a cross-sectional radius r is considered. The degradation process is delineated into two stages. Initially, in the first stage, microcracks and other defects emerge within the material due to the applied force F during the initial loading period. The dissolution occurring in the time interval $0 \leq \tau \leq t_0$ is referred to as the latent dissolution stage, during which the material retains its functionality. Subsequently, in the second stage $t_0 \leq \tau \leq t^*$, the microcracks and defects formed in the earlier stage coalesce, forming macrocracks that systematically propagate throughout the material's volume. At the critical moment $\tau = t^*$, complete breakdown occurs, rendering the material entirely non-functional. Under these conditions, the damage function $\omega(t)$ can be expressed as $\omega(t_0) = 0$ and $\omega(t^*) = 1$.

With the information provided, it appears that the relationship between stress and strain for uniaxial tension can be expressed using equation (7)

$$\tilde{\varepsilon} = \frac{\tilde{\sigma}}{E(1-\omega(t))}. \quad (8)$$

The relationship between stress and strain for hereditary media can be expressed as follows (Chertishchev, 2020).

$$\tilde{\varepsilon} = \frac{1}{E} \left(\tilde{\sigma}(t) + \int_0^t B(\tau) \tilde{\sigma}(\tau) d\tau \right). \quad (9)$$

Classical robustness condition

$$\tilde{\varepsilon} \leq [\varepsilon]. \quad (10)$$

In the following manner, the deformation strength limit can be expressed as the stress strength limit through physical dependencies: $[\varepsilon]$ represents the deformation strength limit.

$$[\varepsilon] = \frac{[\sigma]}{E(1-\omega)}. \quad (11)$$

When substituting (7) into (9) and subsequently incorporate (9) and (11) into (12), we arrive at an integral equation of Volterra type as follows

$$\frac{\sigma_0}{1-\omega(t)} + \sigma_0 \int_0^t \frac{B(\tau)}{1-\omega(\tau)} d\tau = \frac{[\sigma]}{1-\omega(t)} \quad (12)$$

or

$$(1 + B^*) \tilde{\sigma}(\tau) = \frac{[\sigma]}{1-\omega(t)}. \quad (13)$$

In this context, B^* represents the integral operator that characterizes the damage process and $B(\tau)$ is the kernel of this operator.

$$B^* \cdot 1 = \int_0^t B(\tau) d\tau. \quad (14)$$

Now, the initial stage of the dissolution process can be analyzed. To do so, employing the criterion approach and assuming the absence of defects in the tube before its use, the expression for the maximum stress in the rod undergoing a homogeneous

stress state, as denoted by equation (14), can be formulated as follows (Piriev, 2023; Akhmedov & Yusubova, 2022)

$$(1 + B^*)\sigma_{max} = [\sigma]. \quad (15)$$

The analysis of formula (1) reveals that the maximum stress for a uniaxial tensile state is represented by the normal stress induced in the cross-section of the rod. Consequently, the initial damage will be caused by this tensile stress

$$\sigma_{max} = \frac{F}{A_0}. \quad (16)$$

Expressing formula (15) in terms of the damage criterion results in the following algebraic equation for determining the initial damage time

$$\int_0^{t_0} B(\tau) d\tau = g - 1. \quad (17)$$

Here $g = \frac{[\sigma]}{\sigma_0}$.

The initial damage time for the three forms of the kernel $B(\tau)$ included in the derived equation (17) is determined as follows (Slavin *et al.*, 2022)

$$B(t) = 1; \quad t_0 = g - 1, \quad (18)$$

$$B(t) = e^{-\alpha t}; \quad t_0 = \frac{1}{\alpha} \ln[1 + \alpha(g - 1)]^{-1}, \quad (19)$$

$$B(t) = t^{-\alpha}; \quad t_0 = [(1 - \alpha)(g - 1)]^{\frac{1}{1-\alpha}}. \quad (20)$$

The formulas (18)-(20), which determine the initial damage time, show that if the material kernel is singular and stable, dispersion will occur at the lowest tensile force and as this force decreases, the value of t_0 will increase. In the scenario of a standard exponential kernel, the minimum value for the decay time is derived (Piriev, 2023; Akhmedov & Yusubova, 2022; Akhmedov, 2021). It is now imperative to investigate the second phase of the dissolution process. To achieve this, equation (12) can be articulated as follows

$$\int_0^t B(t, \tau) \frac{1}{1-\omega(\tau)} d\tau = \frac{g-1}{1-\omega(t)}, \quad (21)$$

considering the damage operator as a constant $B(t, \tau) = B_0 = const$ and differentiating the integral equation, the solution is examined. This is done by differentiating both sides of equation (21) concerning the

$$\frac{B_0}{1-\omega} = \frac{g-1}{(1-\omega)^2} \frac{d\omega}{dt},$$

or

$$\frac{d\omega}{dt} = \frac{B_0}{g-1} \cdot (1 - \omega). \quad (22)$$

By integrating the differential equation (22) with the initial condition $\omega(t = t_0) = 0$, the damage function is determined as following

$$\omega(t) = 1 - e^{-\frac{B_0}{g-1}(t-t_0)}. \quad (23)$$

We can consider the operator kernel $B(t, \tau) = e^{-\alpha(t-\tau)}$ in equation (12) and find the damage function $\omega(t)$ using a similar approach. To achieve this, the following equation is given (12) in the following form

$$\int_0^t e^{-\alpha(t-\tau)} \cdot \frac{1}{1-\omega(\tau)} d\tau = \frac{g-1}{1-\omega(t)}. \quad (24)$$

The value of the unknown integral included in equation (25) is

$$e^{-\alpha t} \int_0^t \frac{e^{\alpha\tau}}{1-\omega(\tau)} d\tau = \frac{g-1}{1-\omega(t)},$$

or

$$\int_0^t \frac{e^{\alpha\tau}}{1-\omega(\tau)} d\tau = \frac{g-1}{1-\omega(t)} \cdot e^{\alpha t}. \quad (25)$$

By differentiating equation (24)

$$\int_0^t \frac{\partial e^{-\alpha(t-\tau)}}{\partial t} \cdot \frac{1}{1-\omega(\tau)} d\tau + \frac{1}{1-\omega(t)} = \frac{(g-1)}{(1-\omega(t))^2} \frac{d\omega(t)}{dt}$$

or

$$-\alpha e^{-\alpha t} \int_0^t \frac{e^{\alpha\tau}}{1-\omega(\tau)} d\tau + \frac{1}{1-\omega(t)} = \frac{(g-1)}{(1-\omega(t))^2} \frac{d\omega(t)}{dt} \quad (26)$$

and by writing (25) in (26), the following differential equation is achieved

$$\frac{d\omega}{dt} = \frac{1-\alpha(g-1)}{(g-1)} \cdot (1-\omega). \quad (27)$$

2.2. Damage vector parameter

The scalar damage parameter is suitable for simple stress states. However, defects like voids, micropores and microcracks that contribute to the damage process are influenced by the applied loads. Microcracks, for instance, typically propagate perpendicular to the largest principal stress. Their growth disrupts interparticle bonds in polycrystals, ultimately leading to material degradation. A scalar damage parameter is insufficient to describe this type of degradation. In such cases, vector or tensor concepts are employed to accurately represent material breakdown. Research studies using this approach are extensively reviewed in (Ge *et al.*, 2018). In cases of plane stress, the rate of defect accumulation, $\dot{\omega}$, is dependent on the normal stress acting on each plane. When the ω parameter reaches its limit value in any direction, local degradation occurs. Afterward, as the degradation front propagates through the material, complete degradation takes place.

Damage vector parameter for plane stress state,

$$\bar{\omega} = \sqrt{\omega_1^2 + \omega_2^2}, \quad (28)$$

the parameters ω_i and their dependence on head voltages σ_i ($i = 1, 2$) are expressed as follows (Shukla, 2019)

$$\frac{d\omega_i}{dt} = \begin{cases} f(\sigma_i, \omega_i), & \sigma_i > 0, \\ 0, & \sigma_i \leq 0. \end{cases} \quad (29)$$

These dependencies represent the projections of the damage vector in the direction of the principal stresses during the damage process. The damage vector must satisfy the conditions $\bar{\omega}(0) = 0, \bar{\omega}(t^*) = 1$.

The problem of the long-term collapse of a body made of a hereditary type of material in a state of complex stress is considered using the concept of a vectorial parameter of damage.

By considering a prismatic body under plane stress conditions, the areas of the force-acting faces are denoted as A_1, A_2 and the normal stresses acting on these faces are σ_1, σ_2 , respectively ($\sigma_1 \geq \sigma_2$). Using the relationships described in (7), the change in normal stress on each face can be expressed as following

$$\tilde{\sigma}_1(t) = \frac{\sigma_1}{1-\omega_1(t)}; \tilde{\sigma}_2(t) = \frac{\sigma_2}{1-\omega_2(t)}. \quad (30)$$

Now, the generalized Hooke's law for hereditary materials can be expressed as following

$$\begin{cases} \tilde{\varepsilon}_1 = \frac{1}{E^*} \tilde{\sigma}_1 - \frac{\nu^*}{E^*} \tilde{\sigma}_2, \\ \tilde{\varepsilon}_2 = \frac{1}{E^*} \tilde{\sigma}_2 - \frac{\nu^*}{E^*} \tilde{\sigma}_1. \end{cases} \quad (31)$$

The operator form of the material constants in the system of equations (32) can be expressed as follows (Piriev, 2023; Akhmedov & Yusubova, 2022; Akhmedov, 2021)

$$\frac{1}{E^*} = \frac{1}{E} (1 + B^*); \frac{\nu^*}{E^*} = \frac{\nu}{E} (1 + B^*). \quad (32)$$

Here, E represents the modulus of elasticity and ν stands for Poisson's ratio of the material.

After substituting (32) into (31) and utilizing the durability conditions (10) and (11), the durability criteria can be shown as follows

$$\begin{cases} (1 + B^*) \cdot [\tilde{\sigma}_1 - \nu \tilde{\sigma}_2] = \frac{[\sigma]}{1-\omega_1(t)}, \\ (1 + B^*) \cdot [\tilde{\sigma}_2 - \nu \tilde{\sigma}_1] = \frac{[\sigma]}{1-\omega_2(t)}. \end{cases} \quad (33)$$

And by substituting (14) and (30) into (33) and if we differentiate each equation within the system (33) with respect to t , we obtain the following system of equations that involve the components of the damage vector

$$\begin{cases} \frac{1-g_1^{(1)}}{(1-\omega_1)^2} \frac{d\omega_1}{dt} - \nu \frac{g_1^{(2)}}{(1-\omega_2)^2} \frac{d\omega_2}{dt} = \nu \frac{g_1^{(2)}}{1-\omega_2} - \frac{1}{1-\omega_1}, \\ \frac{1-g_2^{(2)}}{(1-\omega_2)^2} \frac{d\omega_2}{dt} - \nu \frac{g_2^{(1)}}{(1-\omega_1)^2} \frac{d\omega_1}{dt} = \nu \frac{g_2^{(1)}}{1-\omega_1} - \frac{1}{1-\omega_2}. \end{cases} \quad (34)$$

Here

$$\begin{aligned} g_1^{(1)} &= \frac{[\sigma]}{\sigma_1}; g_1^{(2)} = \frac{\sigma_2}{\sigma_1}; \\ g_2^{(2)} &= \frac{[\sigma]}{\sigma_2}; g_2^{(1)} = \frac{\sigma_1}{\sigma_2}. \end{aligned}$$

are markings inserted in the form.

For the plane stress state, the system of equations (34) for a qualitative analysis of the damage process is simplified. We'll assume that the normal stresses acting on the faces of a plane body are equal to the areas of those faces.

$$A_1 = A_2 = A; \sigma_1 = \sigma_2 = \sigma.$$

Then, the system of equations (34) will be expressed by an equation.

$$\varepsilon = \frac{1}{E^*} \tilde{\sigma} - \frac{\nu^*}{E^*} \tilde{\sigma},$$

or

$$\int_0^t B(t, \tau) \frac{1}{1-\omega(\tau)} d\tau = \frac{g-1+\nu}{(1-\nu)(1-\omega(t))}. \quad (35)$$

In the case of a constant and exponential kernel, differentiating this equation yields equations similar to equations (22) and (27) for the components of the vector damage parameter:

$$\frac{d\omega}{dt} = \frac{1-\nu}{g-1+\nu} (1-\omega), \quad (36)$$

$$\frac{d\omega}{dt} = \frac{1-\nu-\alpha(g-1+\nu)}{g-1+\nu} (1-\omega). \quad (37)$$

Equations (36) and (37) are differential equations that express the time-dependent behavior of the damage vector projections for constant and exponential kernels, respectively. By integrating these equations, the components of the damage vector for both cases are derived as following:

$$\omega(t) = 1 - e^{-\frac{1-\nu}{g-1+\nu}(t-t_0)}, \quad (38)$$

$$\omega(t) = 1 - e^{-\frac{1-\nu-\alpha(g-1+\nu)}{g-1+\nu}(t-t_0)}, \quad (39)$$

for the specific case the magnitude of the damage vector using equation (28) can be expressed as following:

$$\varpi(t) = \sqrt{2}\omega(t). \quad (40)$$

2.3. Numerical calculation

The qualitative analysis of the damage process was conducted using the derived differential equations. Numerical calculations were carried out according to equations (36) and (37) in the Matlab software package. Figures 1 and 2 represent the results according to equation (36), while Figures 3 and 4 illustrate the outcomes based on equation (37). The graphical representation describes the process of accumulation of adjustment to the initial condition $\omega(t = t_0) = 0$.

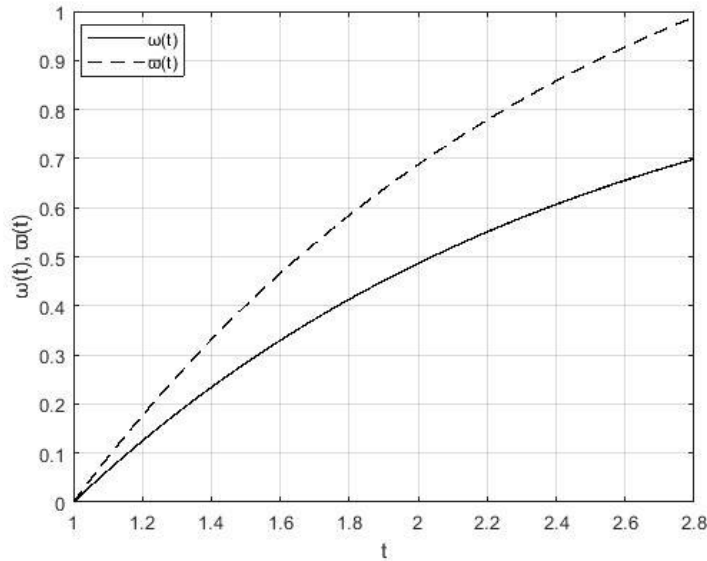


Figure 1. Collection model for damage process for $g = 2$ and $\nu = 0,2$

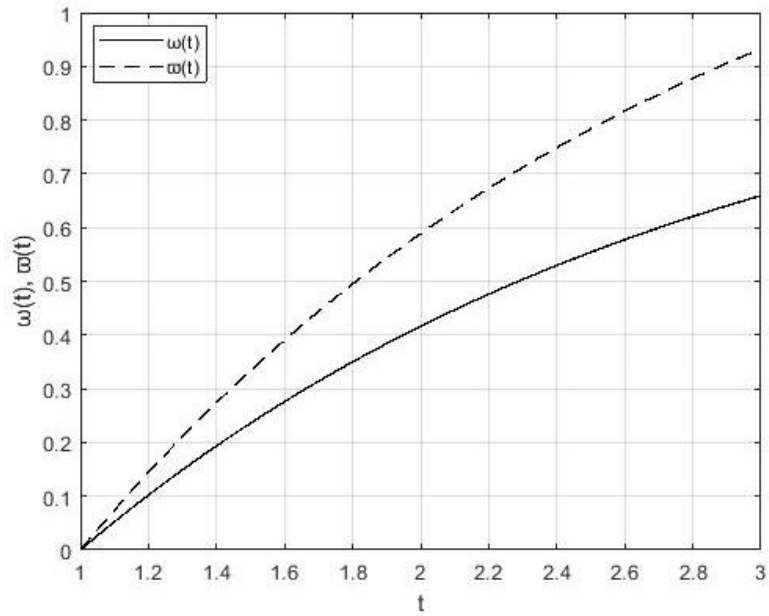


Figure 2. Collection model for damage process for $g = 2$ and $\nu = 0,3$ (b)

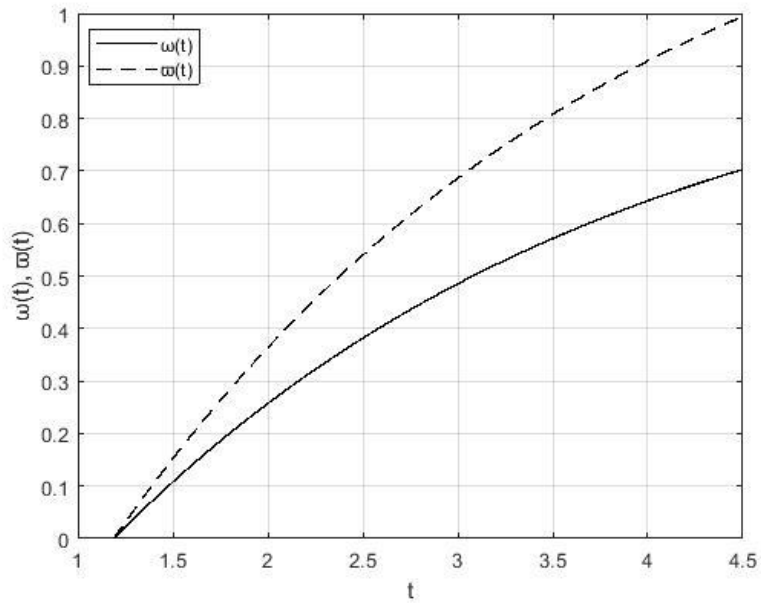


Figure 3. Collection model for damage process for $g = 2$, $\nu = 0,2$ and $\alpha = 0,3$

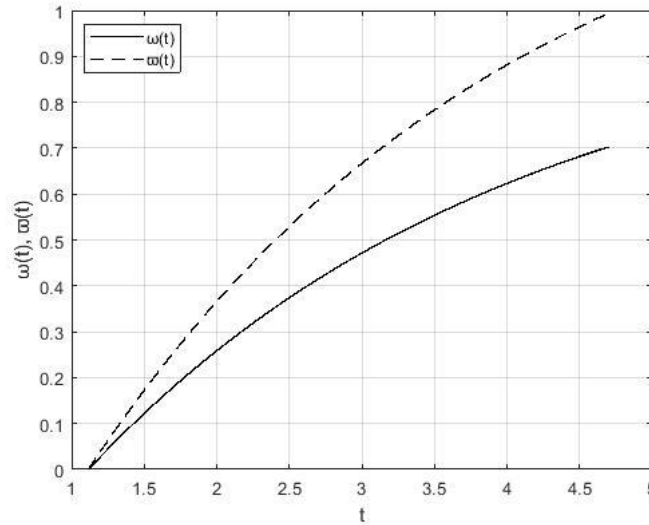


Figure 4. Collection model for damage process for $g = 2$, $\nu = 0,3$ and $\alpha = 0,2$

The analysis of the obtained results reveals that the complete dissolution of the material for a stable core occurs at the moment $t^* = 2.8$ (Figure 1). Initially, considering the value $g = 2$ in equation (18), the latent period of material dissolution (incubation period) is $t_0 = 1$. For $\nu = 0,2$, the critical values of the damage vector and its projections will be $\omega(t^*) \approx 0.6988$, $\varpi(t^*) \approx 1$. For the value $\nu = 0,3$, complete dissolution of the material (critical time) will occur at the moment $t^* = 3$, with the critical values of the damage vector and its projections being $\omega(t^*) \approx 0.6594$, $\varpi(t^*) \approx 1$.

Taking into account the values of $g = 2$, $\nu = 0.2$, $\alpha = 0.3$ for the exponential kernel in (19), the latent decay time (incubation period) of the material is $t_0 = 1.1869$. For these values, solving equation (29) yields $\omega(t^*) \approx 0.7030$, $\varpi(t^*) \approx 1$ as the critical values of the damage vector and its projections. In this case, complete dissolution of the material will occur at time $t^* = 4.5$. Similarly, for $g = 2$, $\nu = 0.3$, $\alpha = 0.2$, complete disintegration of the material will occur at the moment $t^* = 4.6$, with the damage vector and its critical values being $\omega(t^*) \approx 0,7027$, $\varpi(t^*) \approx 1$. According to the results of the mathematical analysis, a piezoelectric device for detecting defects in polymer composite materials is proposed.

3. Piezoelectric device for detecting defects

Based on the analysis of the long-term strength of polymer composite materials, a novel piezoelectric device has been proposed for defect detection (Hasanov *et al.*, 2023). The main advantage and distinctive feature of the proposed piezoelectric device, compared to devices resulting from previous research in this field (Boiprav *et al.*, 2023; Fionov *et al.*, 2023; Vavilov, 2020; 2022; Chulkov, 2023; Chertishchev, 2020; Slavin *et al.*, 2022; Aamir *et al.*, 2019; Ge *et al.*, 2018; Shukla, 2019), lie in its real-time transmission to the layers of the composite material based on coordinates from the transmitting piezoelectric elements arranged in matrices. This design allows for adjustment during the production and operation of composite materials and their components. The device is developed with the capability of providing accurate indication of the location of defects in the composite material based on coordinates. This is achieved by amplifying and comparing small amplitude electric signals received from the receiving

piezo element, organized into matrices corresponding to the amplitude of the electric signals and the signals reflected from the layers of the composite, according to the table of reference signals in the comparison scheme.

The device operation is elucidated by the diagram illustrated in Figure 5.

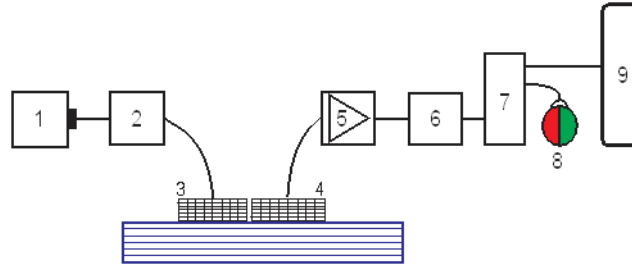


Figure 5. Block diagram of a piezoelectric device designed for detecting defects in polymer composite materials

A piezoelectric device designed for the detection of defects within polymer composite materials is comprised of multiple components: a voltage generator - 1, a connected transmitter - 2, a matrix-divided piezo-element transmitter - 3, a matrix-divided piezo-element receiver - 4, a sumimator - 5, a voltage converter – 6, consisting of an etalon and a comparison circuit for assessing incoming signals during actual measurements - 7, two-color light-emitting diodes (LEDs) that convey normal (green) and alarm (red) states and are connected in parallel to the comparison circuit - 8 and a digital display screen for presenting data - 9.

The operational principle of this proposed piezoelectric defect-detection device for polymer composite materials is as follows: To establish the required signal transmission parameters, the voltage generator – 1, sends signals through the matrix-shaped piezo-element transmitter – 3, into the composite material. Signals initially generated by the transmitter – 2, are conveyed to specific sections of the matrix-divided piezo-element transmitter - 3. The transmitter piezo-element plays a crucial role in determining the presence or absence of defects within the polymer material. The device operates by capturing signal waves reflected from the material, identifying differences in the inner layer of the polymer part (homogeneous or defective) and relaying the data through the matrix-divided piezo-element receiver - 4. Subsequently, input signals received from various matrices are amalgamated into a signal with overall amplitude via the sumimator – 5 and are then transmitted to the voltage converter - 6. The output signal from the voltage converter is directed to the comparator circuit - 7, which consists of two segments for comparing signals under standard and actual measurement conditions. The comparison circuit integrates two-color LEDs – 8, to indicate the device's status. If no defects are detected in the composite material, the green LED is illuminated; however, the red LED activates if there are differences in the incoming signal amplitudes, signifying the presence of defects. The results are displayed on the digital screen - 9. Consequently, this device provides real-time determinations regarding the existence of complex defects within the volume of the composite material and the components created from it.

4. Conclusion

The investigation addresses the issue of scattered destruction of structural elements under both simple and complex stress states, employing the strength criterion for hereditary damaged materials. The determination of the initial moment of destruction (incubation period) is approached through the criterion method, resulting in the construction of differential equations that include a parameter characterizing the destruction process for both stress states. A comparison with classical models reveals that the change in the damage process over time aligns with both models, with the advantage of the newly obtained differential equations incorporating material constants explicitly.

The obtained differential equations for both stress states are linear, they can be solved analytically. The curves representing the scattered destruction process for various material constant values were constructed for the given function $\omega(t)$ through integral integration of the differential equations using the MATLAB package. These solutions offer insights into predicting the durability of diverse structural elements subject to complex stress conditions, considering the influence of a complex stress state on long-term strength through the principal stress.

References

- Aamir, M., Tolouei-Rad, M., Giasin, K. & Nosrati, A. (2019). Recent advances in drilling of carbon fiber-reinforced polymers for aerospace applications: A review. *The International Journal of Advanced Manufacturing Technology*, 105, 2289-2308.
- Akhmedov, N.K. (2021). Axisymmetric problem of the elasticity theory for the radially inhomogeneous cylinder with a fixed lateral surface. *Journal of Applied and Computational Mechanics*, 7(2), 599-610.
- Akhmedov, N.K., Yusubova, S.M. (2022). Investigation of elasticity problem for the radially inhomogeneous transversely isotropic sphere. *Mathematical Methods in the Applied Sciences*, 45(16), 10162-10186.
- Bashirov, R.J., Ismailov, N.E. (2022). Criteria for destruction of polymer composite materials. *Izvestia*, 2(62), 130-142.
- Boiprav, O., Hasanov, M., Bogush, V.A. & Lynkou, L. (2023). Flexible double-layered microwave absorbers based on foiled materials with mechanically treated surface. *New Materials, Compounds and Applications*, 7(2), 100-110.
- Chertishchev, V.Yu. (2020). Development of technologies and means of acoustic impedance control of multilayer honeycomb structures from polymer composite materials: thesis, Cand. Sc. (Tech.). Moscow: Bauman MSTU, 180 (in Russian).
- Chulkov, A.O., Vavilov V., Nesteruk, D., Burleigh D. & Moskovchenko A. (2023). A method and apparatus for characterizing defects in large flat composite structures by Line Scan Thermography and neural network techniques. *Frattura ed Integrita Strutturale*, 63, 110-121.
- Fionov, A., Kraev, I., Yurkov, G., Solodilov, V., Zhukov, A., Surgay, A., Kuznetsova, I. & Kolesov, V. (2022). Radio-absorbing materials based on polymer composites and their application to solving the problems of electromagnetic compatibility. *Polymers (Basel)*, 14(15), 3026.
- Ge, C., Wang, L., Liu, G. & Wang, T. (2018). Enhanced electromagnetic properties of carbon nanotubes and SiO_2 -coated carbonyl iron microwave absorber. *Journal of Alloys and Compounds*, 767, 173-180.
- Hasanov, M.H., Bashirov, R.C. & Ismayilov, N.E. (2023). Piezoelectric device for detecting defects in polymer composite materials. AzPatent No. a20230121.
- Piriev, S.A. (2023). Scattered destruction of a cylindrical isotropic thick pipe in an aggressive medium with a complex stress state. *Engineering Cyber-Physical Systems and Critical*

Infrastructures, 7, 383-395.

Shukla, V. (2019). Review of electromagnetic interference shielding materials fabricated by iron ingredients. *Nanoscale Advances*, 1(5), 1640-1671.

Slavin, A.V., Dalin, M.A., Dikov, I.A., Boychuk, A.S. & Chertishchev, V.Yu. (2021). Current trends in development of acoustic non-destructive testing methods in aviation industry (review). *Trudy VIAM*, 12(106), paper no. 11.

Vavilov, V., Burleigh, D. (2020). *Infrared thermography and thermal nondestructive testing*, 82. New York: Springer International Publishing.

Vavilov, V.P. Chulkov, A.O., Smotrova, S.A., Scherbakov, V.N. & Storozhenko, V.A. (2022). Infrared thermographic analysis of thermal property variations in composites subjected to impact damage, thermal cycling and moisture saturation. *Composite Structures*, 296, 115927.